OSU-TA-7/95

Post Big Bang Processing of the Primordial Elements

M. J. Balbes, R. N. Boyd[1], G. Steigman[1] and D. Thomas
Department of Physics, The Ohio State University, Columbus, OH 43210

ABSTRACT

We explore the Gnedin-Ostriker suggestion that a post-Big-Bang photodissociation process may modify the primordial abundances of the light elements. We consider several specific models and discuss the general features that are necessary (but not necessarily sufficient) to make the model work. We find that with any significant processing, the final D and ^{3}He abundances, which are independent of their initial standard big bang nucleosynthesis (SBBN) values, rise quickly to a level several orders of magnitude above the observationally inferred primordial values. Solutions for specific models show that the only initial abundances that can be photoprocessed into agreement with observations are those that undergo virtually no processing and are already in agreement with observation. Thus it is unlikely that this model can work for any non-trivial case unless an artificial density and/or photon distribution is invoked.

Subject headings: cosmology: theory – early universe – gamma rays: theory – nuclear reactions, nucleosynthesis, abundances

---

[1]Also Department of Astronomy, Ohio State University, Columbus, OH 43210

1. Introduction

The standard model of big bang nucleosynthesis (SBBN)(Peebles 1966; Wagoner, Fowler, & Hoyle 1967; Schramm & Wagoner 1977; Boesgaard & Steigman 1985; Walker et al. 1991) makes well defined predictions of the primordial abundances of the light elements. These predictions agree reasonably well with the commonly accepted values of the primordial element abundances as inferred from observation (Walker et al. 1991; Balbes, Boyd, & Mathews 1993; Smith, Kawano, & Malaney 1993) at a baryon-to-photon ratio of about $\eta \sim 3 \times 10^{-10}$. However, this baryon density corresponds to only a few percent of the closure density of the universe. This result has motivated a number of attempts to reconcile the observed big bang abundances with a model in which η is much larger.

In this context, it was suggested by Gnedin & Ostriker 1992(GO) that a population of black holes may have formed from an early generation of massive stars. The collapse of the stars to black holes does not significantly contaminate the primordial abundances. The black holes then accrete matter and produce a photon bath which further processes the remaining primordial material. GO chose initial SBBN abundances at two values of the baryon-to-photon ratio which are higher than that which agrees with any of the abundance determinations. Thus, they start with an excess of ^{4}He and ^{7}Li and a deficit of D and ^{3}He. The ^{4}He and ^{7}Li are then processed into the lighter elements as a function of the total photon energy input into the system. Although GO are not able to process any significant amounts of ^{4}He, they claim to be in agreement with the observed primordial abundances at the 3σ level. (See also a more recent paper (Gnedin, Ostriker & Rees 1995)).

In this paper we investigate in detail general models of nucleosynthesis induced by post-Big-Bang photoprocessing and determine the conditions under which the observed light element abundances can be reproduced. As we will show, we are unable to find a non-trivial solution where the initial abundances do not already agree with observation. The reason for this is straightforward. The SBBN abundance of ^{4}He is larger, by some 4 or more orders of magnitude, that those of D and/ or ^{3}He (especially at high values of η). It is therefore not possible to destroy enough ^{4}He to achieve consistency with observations without, at the same time, grossly overproducing pregalactic D and/or ^{3}He. Further, at high η, ^{7}Li is significantly overproduced and it is difficult to destroy enough ^{7}Li without destroying too much ^{4}He (and, consequently, overproducing D and ^{3}He). Our detailed calculations will provide support for this simple overview.

2. The Photon Spectrum and Energy-Weighted Cross Sections

In the present scenario, the primordial elements are assumed to be bathed in a photon field for a given exposure time and photon intensity. In order to calculate the nucleosynthesis, it is necessary to know the energy spectrum of the radiation emitted by the black holes. Since such spectra are not observed directly, we look to other accreting objects, such as quasars, which may have similar spectra. Measurements have been made of NGC 4151 (Perotti et al. 1981; Baity et al. 1984) and other quasars (von Ballmoos, Diehl, and Schonfelder 1987) in energy ranges from 2 keV (Baity et al. 1984) up to 100 MeV (Trombka et al. 1977; Fichtel, Simpson, & Thompson 1978).

The photon number spectrum can be parameterized by two power laws, one describing the data below 2–3 MeV and with the form $E^{-1.6}$ (Baity et al. 1984), the other describing the data above 2–3 MeV with the form $E^{-2.7}$ (Rothschild et al. 1983). We are only concerned with energies above 2.2 MeV, the binding energy of the deuteron, and thus only use the higher energy power-law. It should be noted that Gnedin & Ostriker 1992 give a more complicated expression for the γ-ray spectrum in order to describe the full energy range. As we shall see, the choice of γ-ray spectrum does not change our conclusions.

Cross sections for (γ, X) reactions, where X = n, p, d, t, ^{3}He, or α have been measured over most of the energy range of interest. In order to describe the photoerosion process, we first calculate the energy-weighted cross sections (Boyd, Ferland & Schramm 1989)

$$\langle\sigma\rangle = \frac{\int_{2.2MeV}^{\infty} \sigma(E) E^{-2.7} dE}{\int_{2.2MeV}^{\infty} E^{-2.7} dE}. \quad (1)$$

Because of the power-law weighting factor, the energy-weighted cross section is dominated by contributions from the excitation function near threshold. Sparse data exist for photodissociation reactions on the lithium isotopes near threshold, contributing up to a 50% systematic uncertainty in the energy-weighted cross section. Cross sections for photodissociation reactions on ^{4}He, ^{3}He, and D are well determined from threshold up to several tens of MeV. The errors in these measurements are sufficiently small ($< 20\%$) that our conclusions will not be affected by improved measurements of these cross sections. Table 2 contains a summary of the calculated energy-weighted cross sections.

3. Photoprocessing of the Elements

We can describe the evolution of the element abundances locally by

$$\frac{1}{\phi}\frac{d\left(N_i\right)}{dt} = \sum_j \left(N_j\right)\left\langle\sigma_{j+\gamma\rightarrow i}\right\rangle - \left(N_i\right)\left\langle\sigma_{i+\gamma\rightarrow j}\right\rangle \tag{2}$$

where $N_i = N_i(\vec{r},t)$ is the number density (at location $\vec{r}$ and time t) of nuclide i and $\phi = \phi(\vec{r})$ is the time-independent photon flux. We can further generalize Eqn. 2 by writing the number density as $N_i(\vec{r},t) = f_i\left(\phi(\vec{r})t\right)\rho(\vec{r})$, where $\rho(\vec{r})$ is the local matter density. For a time-independent $\rho(\vec{r})$, Eqn. 2 can be rewritten with the f_i replacing the N_i and yielding solutions which are the same to within a dimensional constant.

In general, Eqn. 2 might also include β-decay terms which act as both production and destruction mechanisms. In our case the only unstable nuclides of importance are ^{3}H and neutrons. Reaction cross sections (and thus the energy-weighted cross sections) for photoproduction and photodissociation of ^{3}H are very similar to those for ^{3}He (see Table 2). For neutrons the situation is even simpler since all are assumed to decay to protons without undergoing nuclear reactions. Therefore we treat ^{3}H as ^{3}He and neutrons as protons in our calculations.

The simplest model is to adopt a uniform isotropic γ-ray distribution (i.e. ϕ is constant) and a uniform matter density distribution in Eqn. 2. Such a distribution could be produced by a universe populated with a high density of black holes which tend to smear out the $1/r^2$ dependence of the photon flux from an individual source. Eqn. 2 then describes a set of coupled differential equations which can be evolved forward in time as a function of the "exposure"(ϕt) for each element. Furthermore, the solutions obtained from this simple model can be modified to include effects from non-isotropic photon fluxes or non-uniform density distributions. These effects are folded into the solutions to Eqn. 2 by a weighting procedure of the form

$$\left\langle\frac{N_i}{N_H}\right\rangle = \frac{\int_0^\infty w(x)N_i(x)dx}{\int_0^\infty w(x)N_H(x)dx} \tag{3}$$

where $x = \phi(\vec{r})t$ is the position-dependent exposure. Note that with $w(x) = \delta(x - \phi(\vec{r})t)$ we recover the original local solutions.

We examine the effects of several functional forms for $w(x)$. In the first case we assume that there are two separately processed regions. Then $w(x)$ is simply a sum of two δ functions. In the second case, we have assumed a uniform population of black holes surrounded by a uniform density of matter. Processing of the matter is dominated by the

nearest black hole. Thus the final element abundances are given by a spatial averaging of the processed material. In the third case, we consider not only a distribution of black holes but a density distribution which varies as $1/r^2$ so as to produce a flat rotation curve. From these examples, we reach some general conclusions about the necessary (and artificial) form $w(x)$ must have in order to obtain a viable model.

The criterion for these models to be viable is that the calculated abundances are within the limits determined by the observed light element abundances (see Table 1). We have chosen realistic but generous (2σ or greater) limits so that if a model does fail, the failure is due to the model not to the choice of limits. The standard model of big bang nucleosynthesis is in agreement with our limits for $2.5 \times 10^{-10} < \eta < 4.6 \times 10^{-10}$.

In each of the scenarios mentioned above, we have presented the solutions in two different ways. First, we use initial abundances from standard big bang nucleosynthesis which allows us to parameterize our four initial abundances in terms of the baryon-to-photon ratio η. We can then follow the evolution of the abundances as a function of the exposure, ϕt. Second, since it can be argued that an assumption of the existence of primordial black holes negates the SBBN model and necessitates the use of the inhomogeneous model, we invert the solutions to Eqn. 2 for each of our scenarios. Then using the observed abundances, we can trace the evolution backwards in time to solve for the primordial values as a function of the exposure. Thus we avoid making any assumptions about the isotopic content of the pre-photoprocessed universe.

4. Results

4.1. Isotropic photon flux

We have calculated the abundances of the light elements relative to hydrogen for isotropic exposures $0 \leq \phi t \leq 10^3$ photons/10^{-27} cm^2 starting with initial abundances determined from the SBBN model with $10^{-10} < \eta < 10^{-8}$. Fig. 1 shows the evolution of the abundances as a function of the exposure, ϕt. Horizontal lines represent the observationally inferred abundances. In Fig. 2 we map out the regions of ϕt versus η space where the individual abundances agree with observation. At no values of η and ϕt can the processed abundances of ^{4}He, ^{3}He, and D be reconciled with the observed limits except in the region where the unprocessed abundances already essentially agree with observation. In fact, this scenario can be ruled out by just looking at the ^{4}He and ^{3}He abundances. Since most

^{4}He is being converted directly into ^{3}He and the ^{4}He abundance is so much greater than ^{3}He, any small change in the ^{4}He abundance is accompanied by a very large change in the ^{3}He abundance. This is clearly seen in the figures to be independent of the initial ^{3}He abundance (and therefore also independent of η). Deuterium is constrained to rise more slowly than ^{3}He because its production is predominantly from ^{3}He through the ^{3}He(γ,p)D reaction. Therefore, deuterium production cannot proceed until a significant quantity of ^{3}He has been created.

At large exposures, when most of the ^{4}He has been destroyed, the ^{3}He abundance begins to decrease, eventually reaching agreement with observation. However, this large ϕt scenario is ruled out because the ^{4}He and D abundances are well outside the observational bounds.

We have inverted the solutions to Eqn. 2 in order to calculate the possible combinations of initial abundances for which this model will work. We are therefore no longer constrained by SBBN. Solutions for the initial abundances, which when processed for a given ϕt yield light element abundances in agreement with observations, are found only for $\phi t < 9.1 \times 10^{-3}$ photons/10^{-27} cm^2. Therefore, no significant processing occurs. Indeed, the *initial* ^{4}He and ^{3}He abundances are constrained to be within the observational limits. The initial D abundance can be less than the observed lower limit by only $\sim 5\%$ and cannot be more than the observed upper limit. The initial ^{7}Li abundance can be no more than 0.3% above the upper limit.

4.2. Two-zone model

We have investigated the possibility of reconciling the helium and deuterium isotope abundances by assuming a two-zone model, i. e. $w(x)$ is a sum of two δ functions. This provides a simplified description of a mixture of material processed through different exposures. In this case, space is divided into two regions, one of which undergoes very little or no processing and the other undergoes a great deal of processing. In the former case, deuterium and ^{3}He agree with observation and ^{4}He is overabundant. It is also necessary that $\eta < 10 \times 10^{-10}$ so that deuterium is not underproduced (see Fig. 1). The latter zone undergoes significantly more processing such that most of the ^{4}He is destroyed. Also, the ^{3}He and deuterium which have been created from the processed ^{4}He have been destroyed to such an extent that they once again are close to the observational limits. Then by adjusting the relative volumes of the two zones (such that the larger volume is only slightly processed and the smaller volume is highly processed), one can force agreement between the processed

^{4}He and the observational limits. In the larger mostly-unprocessed zone the ^{3}He abundance constrains $\phi t < 10^{-2}$. The ^{4}He and ^{7}Li are therefore essentially unprocessed. However, since ^{7}Li is overproduced by a greater factor than ^{4}He, and the zone-mixing reduces the ^{7}Li by the same fraction as ^{4}He, the ^{7}Li is still overproduced in this model. The only way to reconcile the model with observation is to start with primordial abundances for ^{7}Li, ^{3}He, and deuterium which agree with the observational limits already. Even then, the primordial ^{4}He cannot be more than a few percent overabundant due to the constraints placed on η by ^{7}Li.

4.3. Uniform black hole distribution

Although the two-zone model shows clearly why agreement cannot be attained between the primordial abundances and observation, it is too simple a model from which to infer general conclusions. In order to investigate a more physical picture, we have studied a model that has a uniform distribution of black holes that are assumed to be weak enough and/or far enough apart that processing of the primordial material is dominated by the closest black hole. In order to account for the spatial variation of the photon flux, we modify Eqn. 2 by setting $\phi(r) = L_\gamma/4\pi r^2$, where L_γ is the total γ-ray luminosity from one accreting black hole. We can then write the spatially-averaged abundance relative to hydrogen as

$$\left\langle \frac{N_i}{N_H} \right\rangle = \frac{\int_{R_{min}}^{R_{max}} N_i \left(\frac{L_\gamma t}{4\pi r^2}\right) r^2 dr}{\int_{R_{min}}^{R_{max}} N_H \left(\frac{L_\gamma t}{4\pi r^2}\right) r^2 dr} = \frac{\int_{R_{min}}^{R_{max}} f_i \left(\frac{L_\gamma t}{4\pi r^2}\right) \rho(r) r^2 dr}{\int_{R_{min}}^{R_{max}} f_H \left(\frac{L_\gamma t}{4\pi r^2}\right) \rho(r) r^2 dr}. \tag{4}$$

We examine two cases in detail. In the first case, we assume that $\rho(r)$ is constant, i.e. the matter is distributed homogeneously. Then Eqn. 4 can be written more conveniently in terms of one parameter $x = \frac{L_\gamma t}{4\pi r^2}$ to yield

$$\left\langle \frac{N_i}{N_H} \right\rangle = \frac{\int_{x_{min}}^{x_{max}} f_i\left(x\right) x^{-5/2} dx}{\int_{x_{min}}^{x_{max}} f_H\left(x\right) x^{-5/2} dx}. \tag{5}$$

Alternatively, if we assume that the density of matter falls off with distance from the central source as $\rho(r) = \rho_0(\frac{R}{r})^2$ (which will yield the flat rotation curves seen in galaxies) then Eqn. 4 becomes

$$\left\langle \frac{N_i}{N_H} \right\rangle = \frac{\int_{x_{min}}^{x_{max}} f_i\left(x\right) x^{-3/2} dx}{\int_{x_{min}}^{x_{max}} f_H\left(x\right) x^{-3/2} dx}. \tag{6}$$

Figures 3 and 4 show the dependence of the abundances on x_{min} (with $x_{max} = \infty$ so that $R_{min} = 0$) for three values of η. Figures 5 and 6 illustrate the regions of $\eta - x_{min}$ space where the spatially-averaged abundances agree with observation. It is clearly seen that there is no region of parameter space where the models agree with the observed abundances of ^{4}He, ^{3}He, and D simultaneously except where the standard model (for low baryon density) already works. We have also searched for solutions for $x_{min} < x_{max} < \infty$, where processed material with exposure greater than x_{max} is assumed to be swallowed by the black hole and thus does not contribute to the spatial average. No non-trivial solutions were found.

As with the isotropic photon flux scenario, we have inverted the solutions to Eqns. 5 and 6 in order to calculate the possible combinations of initial abundances for which these models will succeed. Solutions for the initial abundances, which when processed yield light element abundances in agreement with observations, are found only for $\phi t < 3 \times 10^{-3}$ and $\phi t < 8 \times 10^{-6}$ photons/10^{-27} cm^2 for the uniform density and the flat rotation curve models, respectively. Again, no significant processing occurs and the *initial* ^{4}He and ^{3}He abundances are constrained to be within the observed limits. The initial D abundance may be less than the observed lower limit by only $\sim 5\%$ and it cannot be higher than the observed upper limit. The initial ^{7}Li abundance can be no more than 0.3% above the upper limit.

It might be thought that the detailed shape of the photon spectrum will affect the present results. However, changing the power law index or using the parameterization of GO causes only small changes in the energy-weighted cross sections. In the GO case, the energy-weighted cross sections are increased by no more than a factor of 4 even when using the most extreme distortion of the spectrum. Furthermore, changes in the spectra change all the energy-weighted cross sections in the same direction, so the effect on resulting abundances is less than that on the cross sections. Since our conclusions are based on qualitative conflicts between observations and the model predictions, it is not likely that uncertainties in the photon spectrum will affect our conclusions.

4.4. A general solution?

So far we have provided examples of models that don't work. Is it possible to construct a non-trivial model that will work? That is, can we construct a weighting function $w(x)$ (see Eqn. 3) that will reconcile the solutions to Eqn. 2 (shown in Fig. 1) with the observed limits? In constructing such a model, two important features must be kept in mind. First, the weighting function must preferentially mix regions such that a larger fraction of ^{7}Li is destroyed than of ^{4}He. Since the destruction cross section for ^{7}Li is higher than for ^{4}He,

this may be possible. Second, the weighting function must avoid appreciable contributions from the region $10^{-2} < \phi t < 5 \times 10^2$ in order to avoid overproducing ^{3}He and D. As a result, such a function is forced to be of the form shown in Fig. 7. This bimodal distribution is decidedly ad hoc! But, even with a weighting function of this type, it is difficult (and perhaps impossible) to reproduce the observed primordial abundances of D, ^{3}He, ^{4}He, and ^{7}Li.

5. Conclusions

We have investigated several scenarios in which the primordial abundances of the light elements undergo photoprocessing due to a population of γ-emitting objects such as accreting black holes (GO). In all cases, the primordial ^{4}He abundance is constrained to agree with observation since even a small amount of processing of ^{4}He increases the ^{3}He and D abundances by several orders of magnitude. At large exposures, when destruction of ^{3}He and D has occurred, their abundances relative to hydrogen become independent of initial values and cannot simultaneously be reconciled with observation. A general solution which would correct for this effect must preferentially weight the processed regions in such a way as to be pathological.

In short, we find no non-trivial solution to any of the several photodissociation models considered for either SBBN or inhomogeneous BBN abundances corresponding to large values of η. Post BBN photoprocessing of the light elements cannot weaken the upper bound on the universal density of baryons.

This work was supported in part by National Science Foundation grant PHY92-21669 and Department of Energy grant DE-AC02-76ER01545.

REFERENCES

Baity, W. A., Mushotzky, R. F., Worrall, D. M., Rothschild, R. E., Tennant, A. F., Primini, & F. A. 1984, ApJ, 279, 555

Balbes, M. J., Boyd, R. N., & Mathews, G. J. 1993, ApJ, 418, 229

Balestra, F., Busso, L., Garfagnini, R., Piragino, G., & Zanini, A. 1979, Nouvo Cimento, 49, 575

Barnes, C. A., Chang, K. H., Donoghue, T. R., Rolfs, C., & Kammeraad, J. 1987, Phys. Lett. B, 197, 315

Berman, B. L., Faul, D. D., Meyer, P., & Olson, D. L. 1980, Phys.Rev.C, 22, 2273

Bernabei, R., Chisholm, A., d'Angelo, S., de Pascale, M., P., Picozza, P., Shaerf, C., Belli, P., Casano, L., Incicchitti, A., Prosperi, D., & Girolami, B. 1988, Phys.Rev.C, 38, 1990

Boesgaard, A. M. & Steigman, G. 1985, ARA&A, 23, 319

Boyd, R. N., Schramm, D. N., & Ferland, G. J. 1989, ApJ, 336, L1

Burzynski, S., Czerski, K., Marcinkowski, A., & Zupranski, P. 1987, Nucl. Phys., A473, 179

Dietrich, S. S., & Berman, B. L. 1988, Atomic Data and Nuclear Data Tables, 38, 199

Faul, D. D., Berman, B. L., Meyer, P., & Olson, D. L. 1981, Phys.Rev.C, 24, 849

Feldman, G., Balbes, M. J., Kramer, L. H., Williams, J. Z., Weller, H. R., & Tilley, D. R. 1990, Phys.Rev.C, 42, R1167

Fichtel, C. E., Simpson, G. A. & Thompson, D. J. 1978, ApJ, 222, 833

Gnedin, N. Y., & Ostriker, J. P. 1992, ApJ, 400, 1

Gnedin, N. Y., Ostriker, J. P., & Rees, M. J. 1995, ApJ, 438, 40

Gregory, A. G., Sherwood, T. R., & Titterton, E. W. 1962, Nucl. Phys., 32, 543

Griffiths, G. M., Morrow, R. A., Riley, P. J., & Warren, J. B. 1961, Can. J. Phys., 39, 1397

Junghans, G., Bangert, K., Berg, U. E. P., Stock, R., & Wienhard, K. 1979, Z. Phys., A291, 353

Olive, K. A. & Steigman, G. 1995, ApJS, 97, 49

Peebles, P.J.E. (1966) Phys. Rev. Lett. 16, 410

Perotti, F., Della Ventura, A., Villa, G., Di Cocco, G., Bassani, L., Butler, R. C., Carter, J. N., & Dean, A. J. 1981, ApJ, 247, L63

Pinsonneault, M. H., Deliyannis, C. P. & Demarque, P. 1992, ApJS, 78,179

Robertson, R. G. H., Dyer, P., Warner, R. A., Melin, R. C., Bowles, T. J., McDonald, A. B., Ball, G. C., Davies, W. G., & Earle, E. D., 1981, Phys.Rev.Lett, 47, 1867

Rothschild, R. E., Mushotzky, R. F., Baity, W. A., Gruber, D. E., Matteson, J. L., & Peterson, L. E. 1983, ApJ, 269, 423

Schramm, D. N., & Wagoner, R. V. 1977, Ann. Rev. Nucl. Part. Sci. 27, 37

Segrè, E. 1964, Nuclei and Particles (New York, NY: W. A. Benjamin, Inc.)

Skopik, D. M., Asai, J., Tomusiak, E. L., & Murphy II, J. J. 1979, Phys.Rev.C, 20, 2025

Smith, M. S., Kawano, L. H., & Malaney, R. A. 1993, ApJS, 85, 219

Songaila, A., Cowie, L. L., Hogan, C. J., & Rugers, M. 1994, Nature, 368, 599

Ticcioni, G., Gardiner, S. N., Matthews, J. L., & Owens, R. O. 1973, Phys. Lett., 46B, 369

Trombka, J. I., Dyer, C. S. Evans, L. G., Bielefeld, M. J., Seltzer, S. M., & Metzger, A. E. 1977, ApJ, 212, 925

von Ballmoos, P., Diehl, R., & Schonfelder, V. 1987, ApJ, 312, 134

Wagoner, R. V., Fowler, W. A., & Hoyle, F. 1967, ApJ, 148,3

Walker, T. P., Steigman, G., Schramm, D. N., Olive, K. A., & Kang, H. 1991, ApJ, 376, 51

Ward, L., Tilley, D. R., Skopik, D. M., Roberson, N. R., & Weller, H. R. 1981, Phys.Rev.C, 24, 317

Fig. 1.— Abundances relative to hydrogen of the light elements as functions of exposure, ϕt. The initial abundances are calculated from SBBN with $\eta_{10} = 3$ (solid curve), $\eta_{10} = 10$ (dashed curve), and $\eta_{10} = 100$ (dashed-dotted curve). Horizontal lines indicate observational limits on the primordial abundances.

Fig. 2.— Parameter space for the isotropic photon flux model. Hatched areas indicate agreement between the calculated and observed elemental abundance. Vertical hatching is D, hatching with a positive slope is ^{3}He, and hatching with a negative slope is ^{4}He. The region where ^{7}Li agrees with observation is not shown, however it also overlaps the region of agreement between the other three light elements.

Fig. 3.— Abundances relative to hydrogen of the light elements when spatially averaged over a uniform density distribution and a photon flux which decreases as $1/\mathrm{r}^2$. The abscissa is x_{min}, where $x = Lt/4\pi R^2$. The initial abundances are calculated from SBBN with $\eta_{10} = 3$ (solid curve), $\eta_{10} = 10$ (dashed curve), and $\eta_{10} = 100$ (dashed-dotted curve). Horizontal lines indicate observational limits on the primordial abundances.

Fig. 4.— Abundances relative to hydrogen of the light elements when spatially averaged over a density distribution and a photon flux both of which decrease as $1/\mathrm{r}^2$. The abscissa is x_{min}, where $x = Lt/4\pi R^2$. The initial abundances are calculated from SBBN with $\eta_{10} = 3$ (solid curve), $\eta_{10} = 10$ (dashed curve), and $\eta_{10} = 100$ (dashed-dotted curve). Horizontal lines indicate observational limits on the primordial abundances.

Fig. 5.— Parameter space for the spatially-averaged model with a uniform density distribution. Hatched regions indicate where the calculated abundances of D, ^{3}He, and ^{4}He agree with observation. Vertical hatching is D, hatching with a positive slope is ^{3}He, and hatching with a negative slope is ^{4}He. The only agreement for all three abundances occurs in the region of parameter space where the standard (low baryon density) model already works. The region where ^{7}Li agrees with observation is not shown, however it also overlaps the region of agreement between the other three light elements.

Fig. 6.— Parameter space for the spatially-averaged model with a matter density which varies as $1/r^2$. Hatched regions indicate where the calculated abundances of D, ^{3}He, and ^{4}He agree with observation. Vertical hatching is D, hatching with a positive slope is ^{3}He, and hatching with a negative slope is ^{4}He. The only agreement for all three abundances occurs in the region of parameter space where the standard (low baryon density) model already works. The region where ^{7}Li agrees with observation is not shown, however it also overlaps the region of agreement between the other three light elements.

Fig. 7.— Possible weighting function $w(x)$ (thick line) superimposed over the abundance vs. exposure curve for ^{3}He.

Table 1: Observational limits on primordial abundances.

	Abundance Limit	Reference
^{7}Li/H	$< 7 \times 10^{-10}$	1, 2, 3
Y_p	0.215 – 0.244	1, 2, 4, 5
^{3}He/H	$< 2 \times 10^{-5}$	1
D/H	1.2 – 10 $\times 10^{-5}$	1, 2

References. — 1) Walker et al. 1991, 2) Smith, Kawano, & Malaney 1993, 3) Pinsonneault, Deliyannis, & Demarque 1992, 4) Balbes, Boyd, & Mathews 1993 5) Olive & Steigman 1995

Table 2: Energy-weighted cross sections

Reaction	$< \sigma >$ (mb)	Reference
^{7}Li(γ, n)^{6}Li	0.0486	1
^{7}Li(γ, p)^{6}He	0.0480	2, 3
^{7}Li(γ, d)^{5}He	0.0118	2
^{7}Li(γ, t)^{4}He	0.1760	2, 4, 5, 6
^{6}Li(γ, n)^{5}Li	0.1748	1
^{6}Li(γ, p)^{5}He	0.4334	2
^{6}Li(γ, d)^{4}He	0.0047	7
^{6}Li(γ, t)^{3}He	0.0147	2
^{4}He(γ, n)^{3}He	0.0153	8, 9, 10
^{4}He(γ, p)^{3}H	0.0167	8, 11
^{4}He(γ, d)D	7.7×10^{-5}	12
^{4}He(γ, pn)D	0.0013	13
^{3}He(γ, n)pp	0.0547	14
^{3}He(γ, p)D	0.0913	15
^{3}H(γ, n)D	0.0547	14
^{3}H(γ, p)nn	0.0788	14
D(γ, p)n	1.7473	16

References. — 1) Dietrich & Berman 1988, 2) Junhgans et al. 1979, 3) Gregory, Sherwood, & Titterton 1962, 4) Griffiths et al. 1961, 5) Burzynski et al. 1987, 6) Skopik et al. 1979, 7) Robertson et al. 1981, 8) Feldman et al. 1990, 9) Ward et al. 1981, 10) Berman 1980, 11) Bernabei 1988 12) Barnes et al. 1987, 13) Balestra et al. 1979, 14) Faul et al. 1981, 15) Ticcioni et al. 1973 16) Segrè 1964

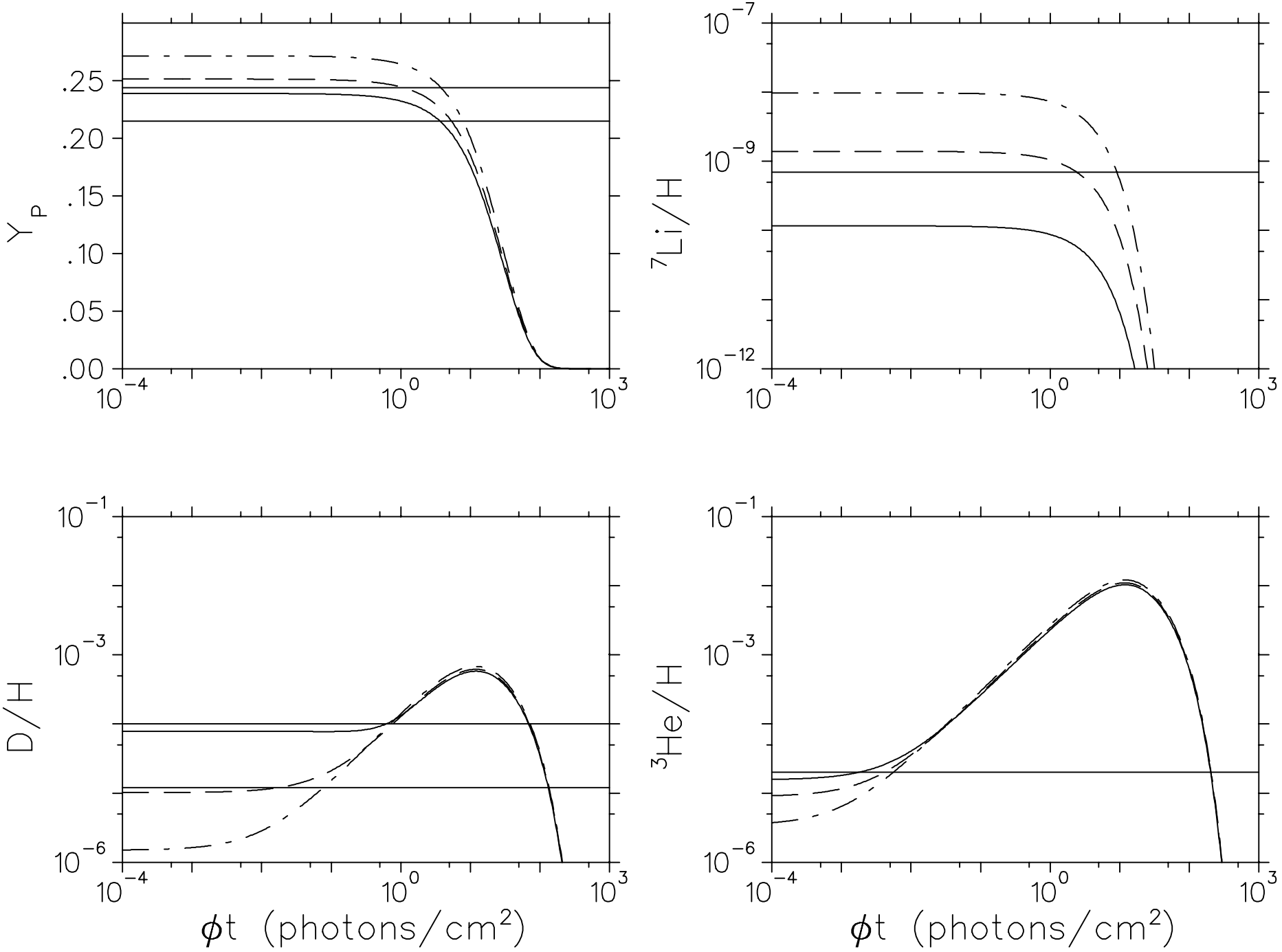
Y_P
.25
.20
.15
.10
.05
.00
10^{-4}
10^{0}
10^{3}
$^7Li/H$
10^{-7}
10^{-9}
10^{-12}
D/H
10^{-1}
10^{-3}
10^{-6}
$^3He/H$
ϕt (photons/cm^2)

ϕt (10^{27} photons/cm^2)
10^{-4}
10^{0}
10^{4}
10^{-10}
10^{-9}
10^{-8}
μ

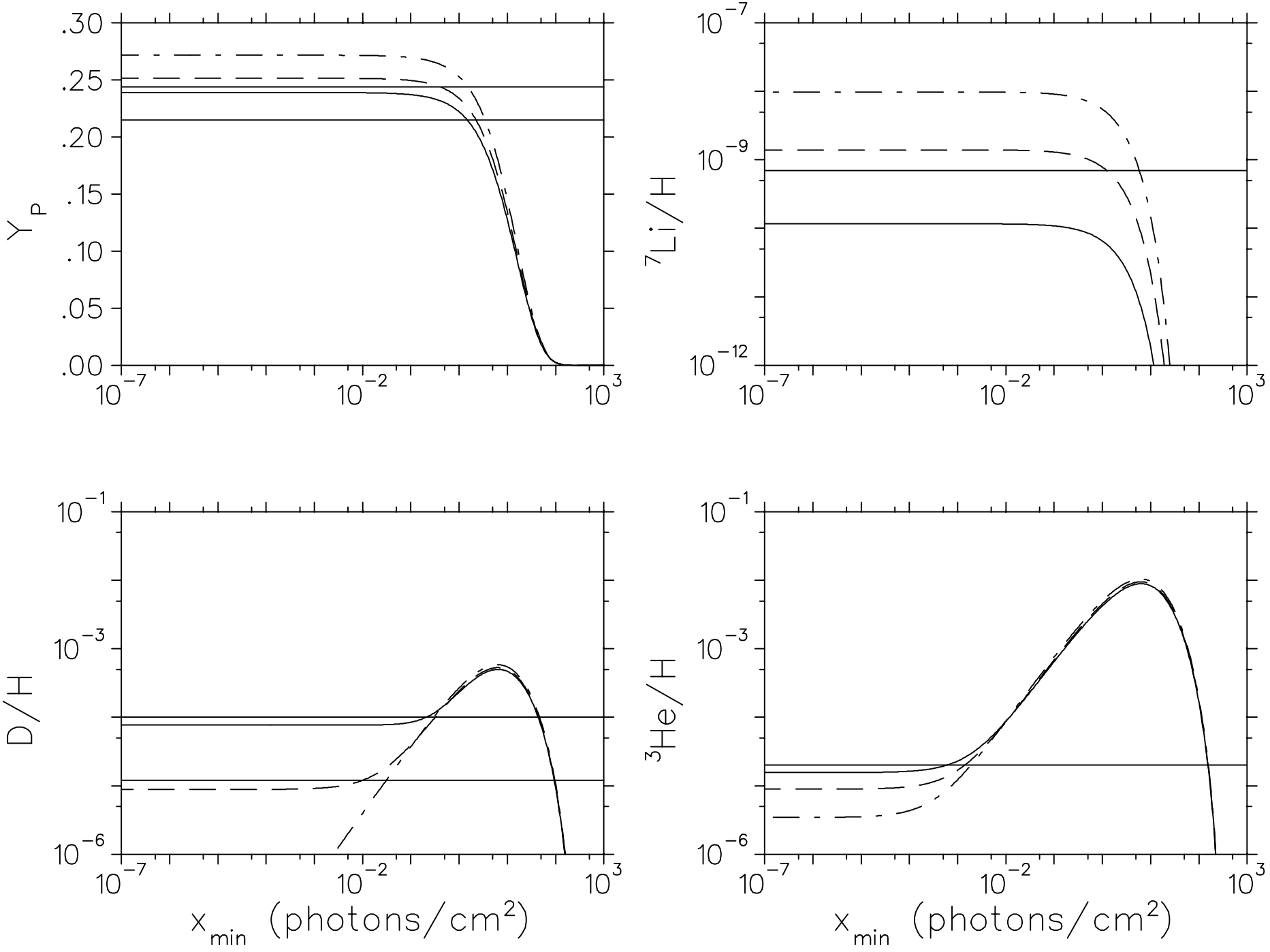
.30
.25
.20
.15
.10
.05
.00
Y_P
10^{-7}
10^{-2}
10^{3}
10^{-7}
10^{-9}
10^{-12}
$^7Li/H$
10^{-1}
10^{-3}
10^{-6}
D/H
x_{min} (photons/cm^2)
$^3He/H$

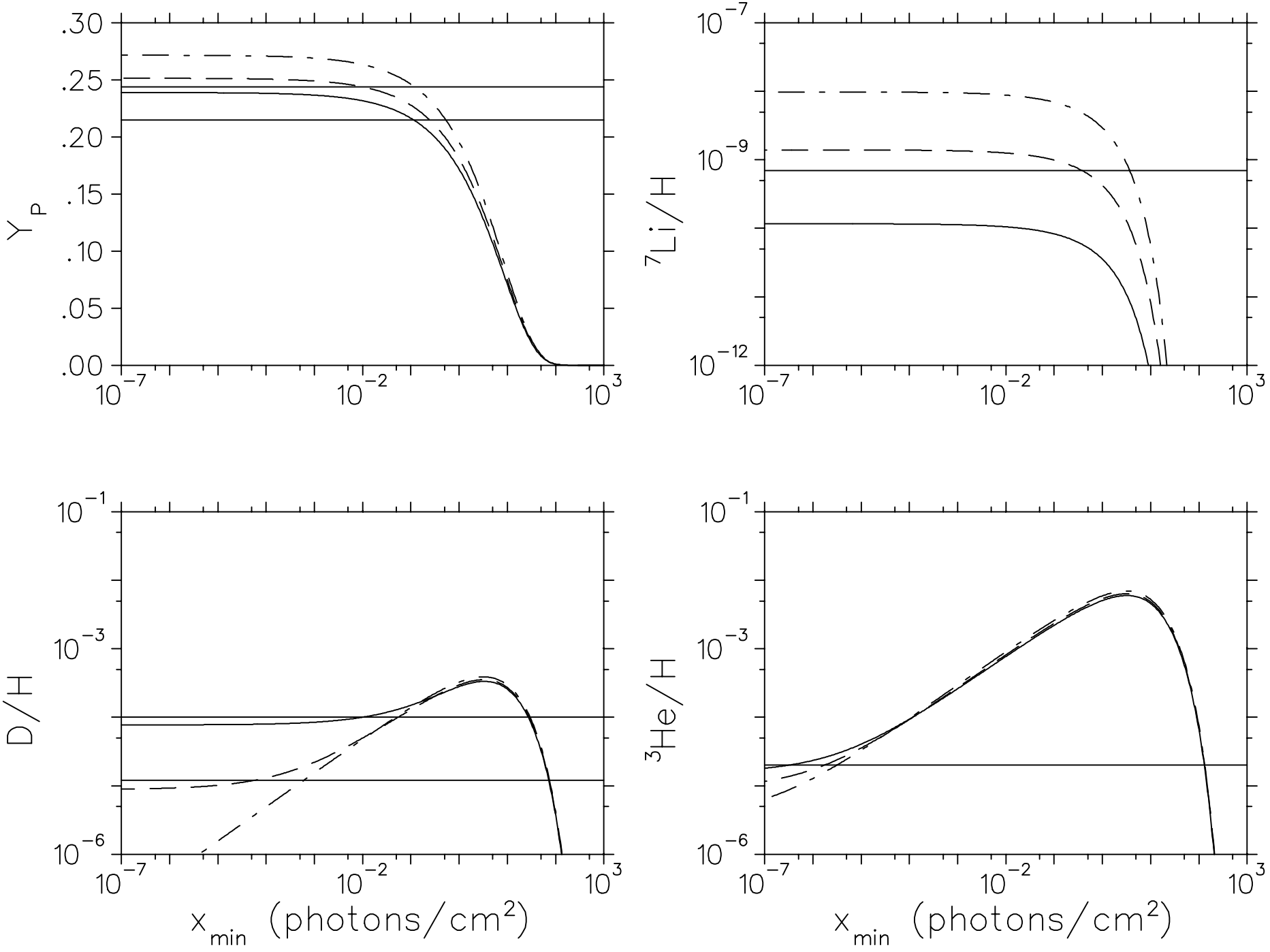
.30
.25
.20
.15
.10
.05
.00
Y_P
10^{-7}
10^{-2}
10^{3}
10^{-7}
10^{-9}
10^{-12}
$^7Li/H$
10^{-1}
10^{-3}
10^{-6}
D/H
x_{min} (photons/cm^2)
$^3He/H$

x_{min} (10^{27} photons/cm^2)
10^{-7}
10^{-2}
10^{3}
10^{-10}
10^{-9}
10^{-8}
μ

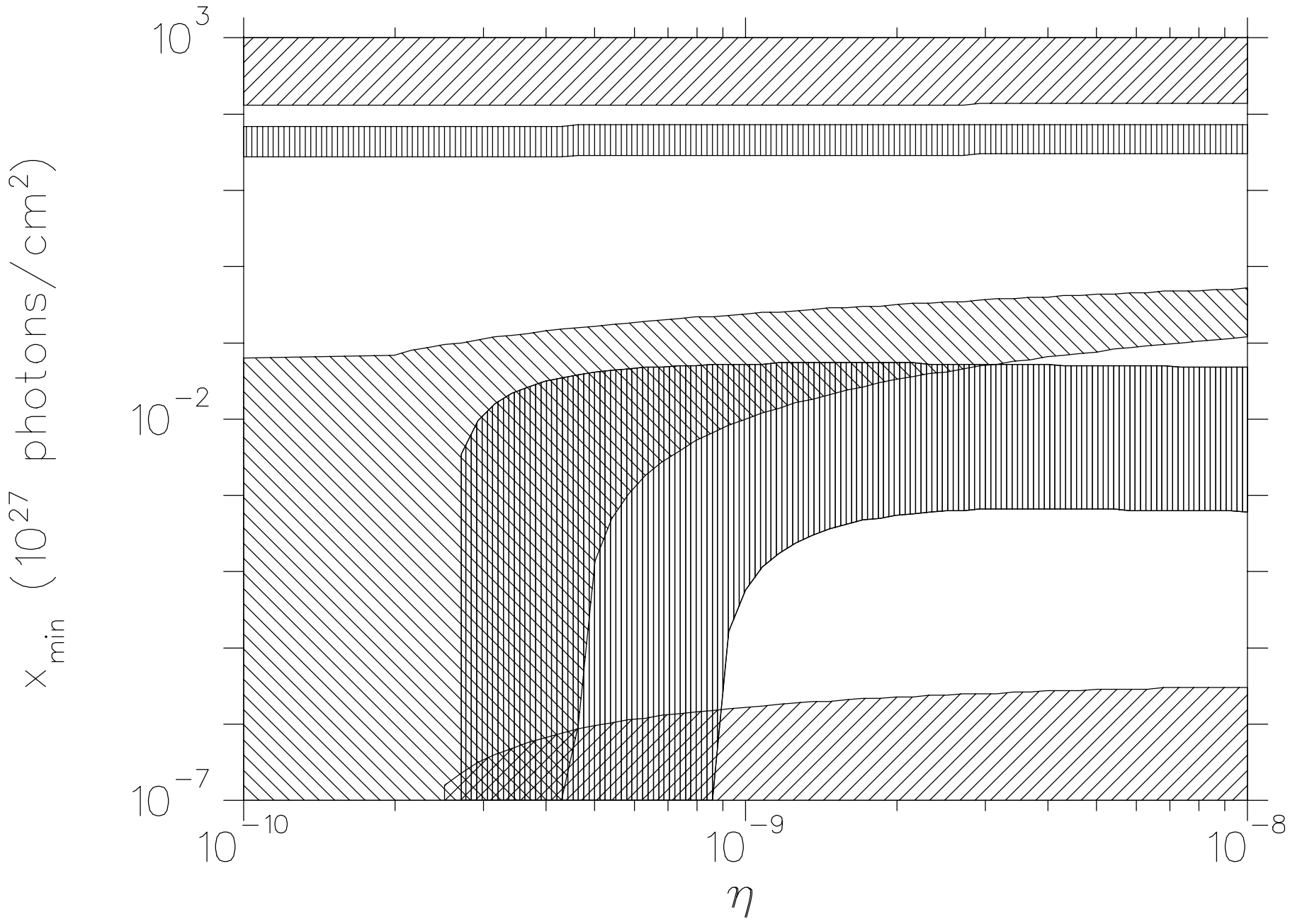
10^{3}
10^{-2}
10^{-7}
x_{min} (10^{27} photons/cm^2)
10^{-10}
10^{-9}
10^{-8}
η

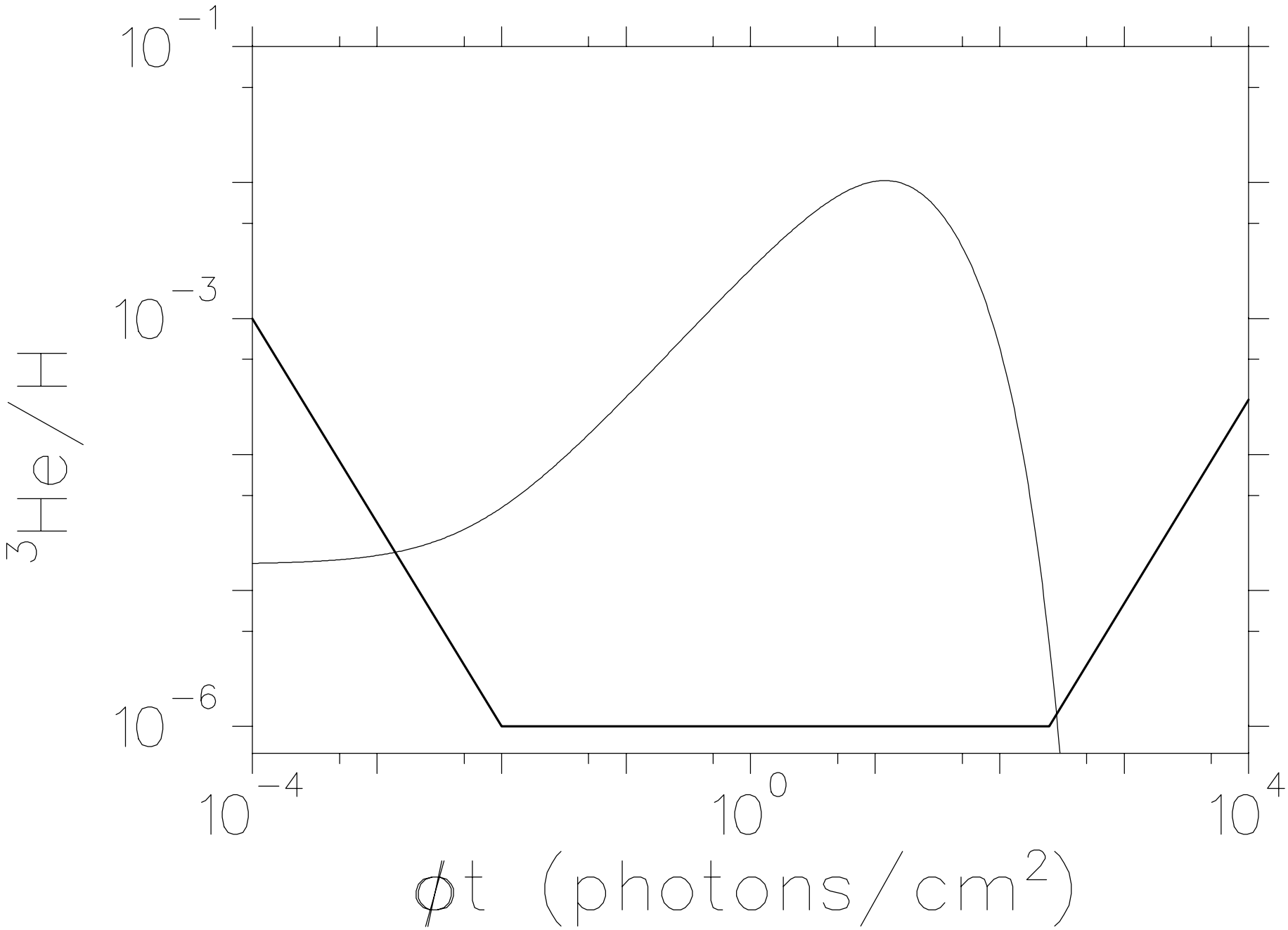
10^{-1}
10^{-3}
10^{-6}
$^3He/H$
10^{-4}
10^{0}
10^{4}
ϕt (photons/cm^2)